



Experimental assessment of the structure-borne noise in an aircraft cabin due to vibrating equipment

Olivier Doutres^{a)}

Department of Mechanical Engineering, École de technologie supérieure, 1100 rue Notre-Dame Ouest, Montréal, Québec, H3C 1K3, Canada

Alexis Caron l'Ecuyer

Core Technical Engineering, Bombardier Aerospace, Montréal, Québec, Canada

Thineshan Kathirchelvan

Core Technical Engineering, Bombardier Aerospace, Toronto, Ontario, Canada

Manuel Etchessahar

Core Technical Engineering, Bombardier Aerospace, Montréal, Québec, Canada

The structure-borne noise due to vibrating equipment (e.g., hydraulic pump, transformer rectifier unit, power transfer unit, avionic fan, etc.) could be a significant noise source inside commercial and business aircraft cabins. Thus, it is important to specify proper noise requirements for equipment suppliers. However, this is not as straightforward as it seems since the structure-borne noise generated by the equipment is not only dependent on the vibrating equipment but also on the dynamical behavior of the aircraft structure to which it is attached. This work investigates the potential of a well-known experimental procedure for predicting the noise generated in the cabin using characteristic properties of the vibration source and the receiving structure. The source is characterized by its structural mobility and free velocity. The receiving structure is characterized by its structural mobility and the transfer function between the applied force at the connection points and the acoustic pressure generated inside the cabin. The proposed method is validated from a small scale laboratory setup comprising of an avionic fan mounted onto an aluminum structure which is then coupled with a small reverberant chamber.

^{a)} email: olivier.doutres@etsmtl.ca

1 INTRODUCTION

The structure borne noise due to vibrating equipment (e.g., pumps, fans, engines etc.) is a subject of concern for acoustic engineers in building, shipping, automotive and aircraft industry for years. The vibrational power of the source is transmitted to the receiver structure through its connections points resulting in annoying acoustic levels if both excitation source and structure connections are not well specified during design phase. Work sharing rules are such that excitation, as a consequence of equipment's operation, is designed by the supplier while the receiving structure, accepting excitation and propagating it through the structure, is designed by the manufacturer. Building¹ and Automotive² industries have developed robust methods to ensure reliable specifications of both excitation and receiver sides. With the reduction of interior noise levels in commercial aircrafts being a concern, aircraft industry also starts using these methods to reduce equipment induced noise³.

The method of interest in this work is based on the characterization of the source active properties (i.e., free velocity or blocked force) and the passive property (i.e., mobility matrix) of both the source and the receiver^{4,5}. All aforementioned properties are measured independently and then combined using straightforward analytical expressions to compute the force at the connection points of the coupled system; this force is commonly referred to as the operational force. Finally, the structure-borne noise (SBN) generated in an acoustic domain (e.g., aircraft cabin) structurally connected to the source is assessed from (1) the operational force and (2) the characterization of the vibro-acoustic transfer function between the pressure generated inside the acoustic domain and a force applied to the receiver structure alone at the location of the connection points.

The objective of this paper is to investigate the potential of this SBN approach for light structures as encountered in aircrafts and coupled to realistic aircraft equipment. This paper focuses on small equipment such as avionic fan, hydraulic pump, transformer rectifier unit inducing tonal noise.

The paper is organized as follow. In section 2, the SBN model based on the source and receiver structure independent properties is presented. The theory is presented in terms of N connection points between the structure and the equipment. It recalls the important parameters to master during design and the various assumptions made so as to simplify the characterization procedure of the sub-structures and be able to propose a simple and practical experimental method. Indeed, only the force and translational displacements along the three orthogonal directions are taken into account (rotational degrees of freedom are neglected). This assumption allows dealing with an engineering method that could be applied by both the aircraft manufacturers and the source suppliers. The SBN method is then applied in section 3 to the case of an avionic fan source hard-mounted onto an aluminum structure which is then coupled with a small reverberant chamber. The SBN effectively measured in two positions inside the reverberant chamber will be compared to the one predicted from the properties of both substructures. The impact of each of the three translational degrees of freedom on the estimated SBN will be investigated.

2 THEORY

2.1 Characteristic properties of the uncoupled elements

Two parameters are required to characterize a SBN source: (1) active properties (i.e., source on) such as the free velocity or the blocked force and (2) passive property (i.e., source off) such

as the mobility or the acceleration^{4,5}. These properties are intrinsic properties of the source and thus do not depend on the structure to which it is attached. In the experimental method used in this work, the receiver structure is only characterized by its structural mobility.

The following subsections define these characteristic properties and briefly describe the experimental methods (or standards) used to measure them.

Passive property: Mobility

The mobility is a characteristic of the dynamical behavior of a structure and characterizes its "ease of motion". It is defined as the complex ratio of the velocity (linear or angular) at one point i of the structure to the force (or moment) excitation applied at point j : $Y_{ij}=v_i/F_j$.

Source and receiver structure mobilities, respectively referred to as Y_S and Y_R , are measured at the N connection points: point mobility for $j=i$ and transfer mobility for $j \neq i$. The boundary conditions of the receiver structure alone (for Y_R measurements) should be the same as the ones set when the source is installed to it and operate in normal conditions. The source mobility is usually measured when the source is freely suspended.

Ideally, six point mobilities are required at each connection point because of the 6 degrees of freedom of both kinematic (linear or angular velocity) and dynamic (force or moment) parameters⁴. Furthermore, it can be expected that what happens in one point is affected by the behaviors of the others. Transfer mobilities should thus be taken into account. Moreover, an interaction may also take place between different components at different points; e.g. the force and velocity components along y at point 1 affect the force and velocity components along z at point 2. Hence, the dimension of the mobility matrices \mathbf{Y}_S and \mathbf{Y}_R should be of size $6N \times 6N$. Note that the bold letters denote matrices or vectors.

In order to avoid a cumbersome and time consuming measurement procedure, only the translational degrees of freedom are characterized; the contributions of moment and angular velocity are neglected. This assumption (1) will allow most of the suppliers to apply the proposed engineering experimental procedure more easily and (2) is not always accompanied by a decrease of the measurement accuracy². The dimension of the mobility matrices \mathbf{Y}_S and \mathbf{Y}_R is thus of size $3N \times 3N$. Furthermore, the transfer mobilities between connection points are accounted for but the transfer mobilities between components (x , y and z) are neglected. In this case, the mobility matrix of dimension $3N \times 3N$ writes:

$$\begin{cases} \mathbf{v}^x \\ \mathbf{v}^y \\ \mathbf{v}^z \end{cases} = \mathbf{Y} \begin{cases} \mathbf{F}^x \\ \mathbf{F}^y \\ \mathbf{F}^z \end{cases} = \begin{bmatrix} \mathbf{Y}^x & [0] & [0] \\ [0] & \mathbf{Y}^y & [0] \\ [0] & [0] & \mathbf{Y}^z \end{bmatrix} \begin{cases} \mathbf{F}^x \\ \mathbf{F}^y \\ \mathbf{F}^z \end{cases}, \quad (1)$$

$$\text{with } \mathbf{v}^p = \begin{cases} v_1^p \\ \vdots \\ v_N^p \end{cases}, \mathbf{F}^p = \begin{cases} F_1^p \\ \vdots \\ F_N^p \end{cases}, \mathbf{Y}^p = \begin{bmatrix} Y_{11}^p & Y_{12}^p & \dots & Y_{1N}^p \\ Y_{21}^p & Y_{22}^p & \dots & \dots \\ \vdots & \vdots & \ddots & \vdots \\ Y_{N1}^p & \dots & \dots & Y_{NN}^p \end{bmatrix} \text{ and } p = x, y, z$$

All components of the mobility matrix are measured according to the standard ISO 7626-5⁶. In the case of the source mobility, measurements are carried out when the source is freely

suspended at the connection points by the use of bungees as described in ISO 7626-2⁷ (see section 5.3 in ref. ⁷).

Active property: free velocity, blocked force

Active properties of the source are measured when the source is operated under normal conditions.

The free velocity \mathbf{v}_f is the velocity at the contact points of the source which, ideally, is not attached to any load or receiver structure. The free velocity is commonly measured when the source is freely suspended at the connection points as documented in the previous section. The only existing standard to assess this property is the ISO 9611⁸. It requires that the source is operated while it is soft-mounted on a rigid support. In the frequency range of the method, the associated restrictions are the following: (1) the vibration at the connection points are not significantly affected by the presence of the selected isolators, flexible connections and foundation, (2) the source supports do behave sufficiently as structure-borne sound point sources (i.e., vibrates as a rigid body). However, the aforementioned free velocity characterization techniques are not adapted for sources creating large forces or moments (e.g., engines, highly unbalanced fan) for which the soft attachments can be destroyed. In this case, the source should be characterized by the blocked force.

The blocked force \mathbf{F}_b is the force injected by the source to a rigid and motionless structure to which it is rigidly attached. Measurement of the blocked force is not straightforward since it requires (1) large test rigs, (2) force sensors (not commonly owned by suppliers) and (3) an infinitely rigid receiver structure. The latter item is an ideal case and is difficult to assess experimentally in a broad frequency range. It is worth noting that, by definition, the blocked force and the free velocity are related to each other by the internal source mobility \mathbf{Y}_s such as:

$$\mathbf{Y}_s = \frac{\mathbf{v}_f}{\mathbf{F}_b}. \quad (2)$$

The blocked force can thus be estimated from measurements of the free velocity and source mobility (but that doesn't solve the problem of characterizing sources creating large forces or moments). The blocked force can also be determined by an indirect method when the source is coupled to a given receiver⁹. This method has been tested but is not presented in this paper.

2.2 "Source/receiver" coupled structure: Operational force and velocity

The source (of mobility \mathbf{Y}_s) and the receiver (of mobility \mathbf{Y}_r) are now connected. Considering a rigid connection assumption, both the source and the receiver move in the same velocity at the contact point location: $\mathbf{v}_s = \mathbf{v}_r = \mathbf{v}_o$. The velocity \mathbf{v}_o is called the "operational velocity". Furthermore, the force applied by the source \mathbf{F}_s and the reaction force of the receiver \mathbf{F}_r are equal in magnitude and opposing each other. Moreover, the force and the velocity at the receiver are linked by the receiver point mobility:

$$\mathbf{Y}_r = \frac{\mathbf{v}_o}{\mathbf{F}_r}. \quad (3)$$

When the sub-structures are coupled, the source can be represented as a blocked force in parallel with an internal impedance $\mathbf{Z}_S = \mathbf{Y}_S^{-1}$ (a Thévenin equivalent source, see ref.⁵). In this case, the force applied to the receiver is given by:

$$\mathbf{F}_R = \mathbf{F}_B - \mathbf{Y}_S^{-1} \mathbf{v}_O. \quad (4)$$

As mentioned in the introduction, the force \mathbf{F}_R is also commonly referred to as the "operational force". Rearranging Eq. (4), the operational force can be written in terms of the source and receiver mobilities and the free velocity:

$$\mathbf{F}_R = (\mathbf{Y}_R + \mathbf{Y}_S)^{-1} \mathbf{v}_f. \quad (5)$$

It can also be written in terms of the blocked force according to Eq. (2):

$$\mathbf{F}_R = (\mathbf{Y}_R + \mathbf{Y}_S)^{-1} \mathbf{Y}_S \mathbf{F}_B. \quad (6)$$

2.3 Structure-borne noise created in an acoustic domain

As mentioned previously, the objective of this work is to predict the noise generated in a given acoustic domain (e.g., aircraft cabin) due to structural vibrations created by a vibrating equipment attached to the aircraft. Because the vibro-acoustic path between the source and the acoustic domain can be extremely complicated, it is characterized in this work by the transfer function H_R defined as the acoustic pressure p created in the acoustic domain due to a force F applied to the receiver structure alone (at source/receiver contact points): $H_R = p/F$. This transfer function can be predicted using elaborated numerical models or assessed experimentally in existing aircrafts. The experimental approach will be used in this work. Tap test is carried out at each connection points along the three directions x , y and z . The vector \mathbf{H}_R of dimension $[3N \times 1]$ is obtained.

The vector \mathbf{p}^{SBN} composed of the acoustic pressure due to each of the N loads along the three directions at the contact points (structure-borne path) is finally assessed from \mathbf{H}_R and the estimation of the force \mathbf{F}_R derived from Eq. (6):

$$\mathbf{p}^{SBN} = \mathbf{H}_R \times \mathbf{F}_R. \quad (7)$$

The total sound pressure level (in dB with a reference acoustic pressure of $2.0e^{-5}$ Pa), referred to as SBN_T , due to the structure-borne contributions at the N contact points is finally computed from the SRSS (square root of the sum of the squares) method applied to Eq. (7):

$$SBN_T = 10 \log_{10} \left(\frac{\sum_{i=1}^{3N} (p_i^{SBN} / \sqrt{2})^2}{p_{ref}^2} \right). \quad (8)$$

It is worth mentioning that Eq. (7) can also be written in terms of the blocked force \mathbf{F}_b . In this case, the transfer function is measured when the source is coupled to the receiver; it is referred to as \mathbf{H}_c in this paper. This transfer function cannot always be measured since it requires that the contact points of the coupled structure be accessible for tap tests.

3 EXPERIMENTAL CASE STUDY: AVIONIC FAN COUPLED TO AN ALUMINUM PANEL RADIATING IN A SMALL REVERBERANT CAVITY

3.1 Description of the experimental setup: reference configuration

The first objective of this work is to validate the formulations presented in the previous section. Specifically, we want to verify that Eq. (8) based on characteristics of the decoupled elements is able to correctly predict the SBN of a vibrating element attached to a receiver. Therefore, a small scale laboratory setup has been designed and is presented in Figure 1. It is based on an avionic fan mounted onto a 1 mm-thick aluminum panel which is then coupled with a small reverberant chamber. The reference indicator is the structure-borne noise created in the cavity at positions M1 and M2 (for microphones 1 and 2 respectively). In the experiment, this indicator is assessed from two measurements for which the source is operating in the same conditions (i.e., fan rotation speed): (1) the acoustic pressure p_{con} when the source is connected to the structure and (2) the acoustic pressure when the source is disconnected p_{discon} . The measured SBN (referred to as SBN_m) is assessed from:

$$SBN_m = 10 \log_{10} \left(\frac{\left(\frac{p_{con}}{\sqrt{2}} \right)^2 - \left(\frac{p_{discon}}{\sqrt{2}} \right)^2}{p_{ref}^2} \right). \quad (9)$$

This laboratory setup has been designed to be representative of configurations usually found in aircrafts: the source is an avionic fan installed perpendicularly to a light aluminum panel using rigid brackets (see Figure 1(d)). As mentioned in section 2.1, linear velocity and force along the three axes at the four connection points CP1-CP4 are characterized. It is worth mentioning that, usually, similar engineering experimental methods³ have been applied in the case of a source directly connected to the radiating structure and only the component normal to it was accounted for (in our work the radiating structure is the aluminum panel and its normal direction is y). However, the source used in this work will create dominant force components along the y and z axis because of the rotating shaft. Both force components should contribute to the SBN in the cavity because the source is mounted in a transverse direction of the vibrating panel. In this work, the impact of the three translational degrees of freedom will be investigated.

3.2 Mobility and vibroacoustic transfer function measurements

Source and receiver mobilities

The experimental setups dedicated to the measurements of the receiver and source mobility matrices are shown in Figure 2. Accelerometers are placed at the four connection points CP1-CP4. Figure 2(a) and 2(b) present the sensors positions for the z and y components measurements of the receiver mobility matrix \mathbf{Y}_R respectively (i.e., \mathbf{Y}_R^z and \mathbf{Y}_R^y in Eq. (1)).

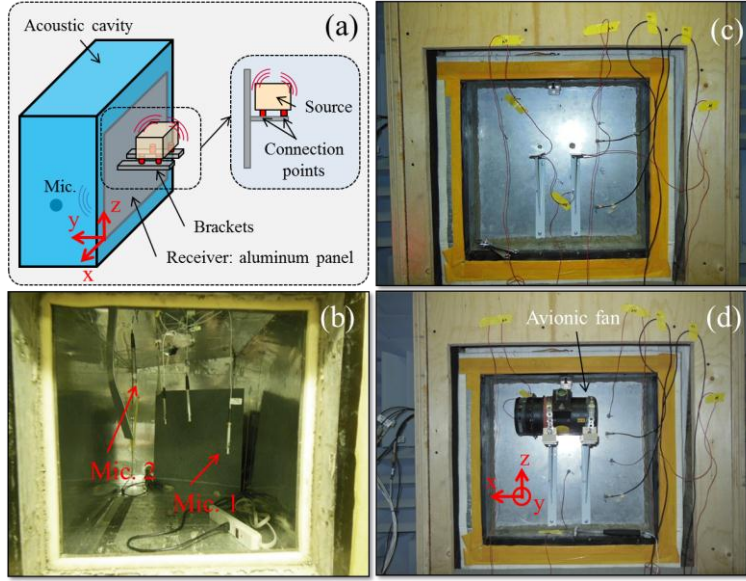


Fig. 1 – (a) Schematic of the coupled structure, (b) interior of the acoustic cavity and position of the microphones, (c) receiver structure alone mounted on the acoustic cavity, (d) source hard-mounted on the receiver structure.

A force impact is applied at the four contact points along the z direction to get \mathbf{Y}_R^z (see Figure 2(a)) and along the y direction to get \mathbf{Y}_R^y (see Figure 2(b)). Figure 2(c) shows the sensors positions for the z component measurements of the source mobility matrix \mathbf{Y}_S (i.e., \mathbf{Y}_S^z in Eq. (1)). The force impact is applied toward z in this case. All mobilities are average mobilities calculated from 10 tap tests. The impact is performed as close as possible from the connection point. Furthermore, the reproducibility of the measurements has been checked.

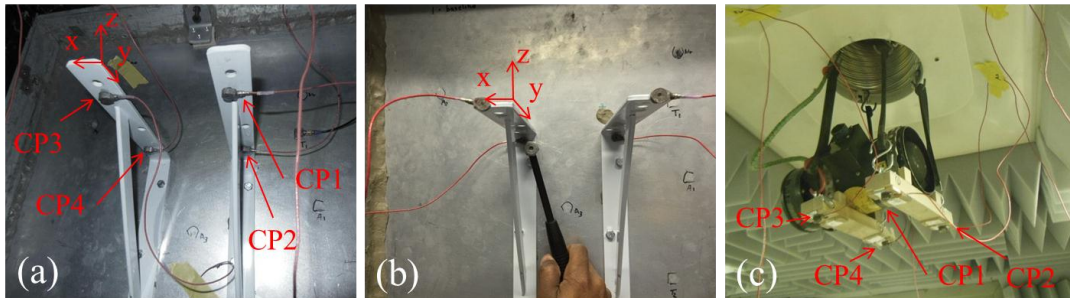


Fig. 2 – Mobility testing; (a) receiver alone $\setminus z$, (b) receiver alone $\setminus y$, (c) source alone freely suspended.

Figure 3(a) and 3(b) show, respectively, the structure and source point mobility measured in the z direction (i.e., $Y_{11}^z, Y_{22}^z, Y_{33}^z$ and Y_{44}^z). It is shown that the mobility of both sub-structures is in the same order of magnitude. As expected, the modal behavior of the receiver structure is more pronounced. Furthermore, the low frequency mobility measured at two connection points CP2 and CP4 is lower compared to the two other points because of the rigid connection between the brackets and the panel. The source point mobility at all connection points is very similar for

frequencies above 400 Hz. Differences at low frequencies between the mobility measured at CP1 and CP2 and the one measured at CP3 and CP4 are not fully explained. They can however be attributed to a different mounting conditions (due to installation) of the two wood pieces onto the avionic fan. Furthermore, Y_S measurements are not straightforward¹ and strongly contribute to the determination of the operational force (see Eqs. (5) and (6)). The accuracy of the source mobility measurements in the low frequency range would have to be more thoroughly investigated in future works.

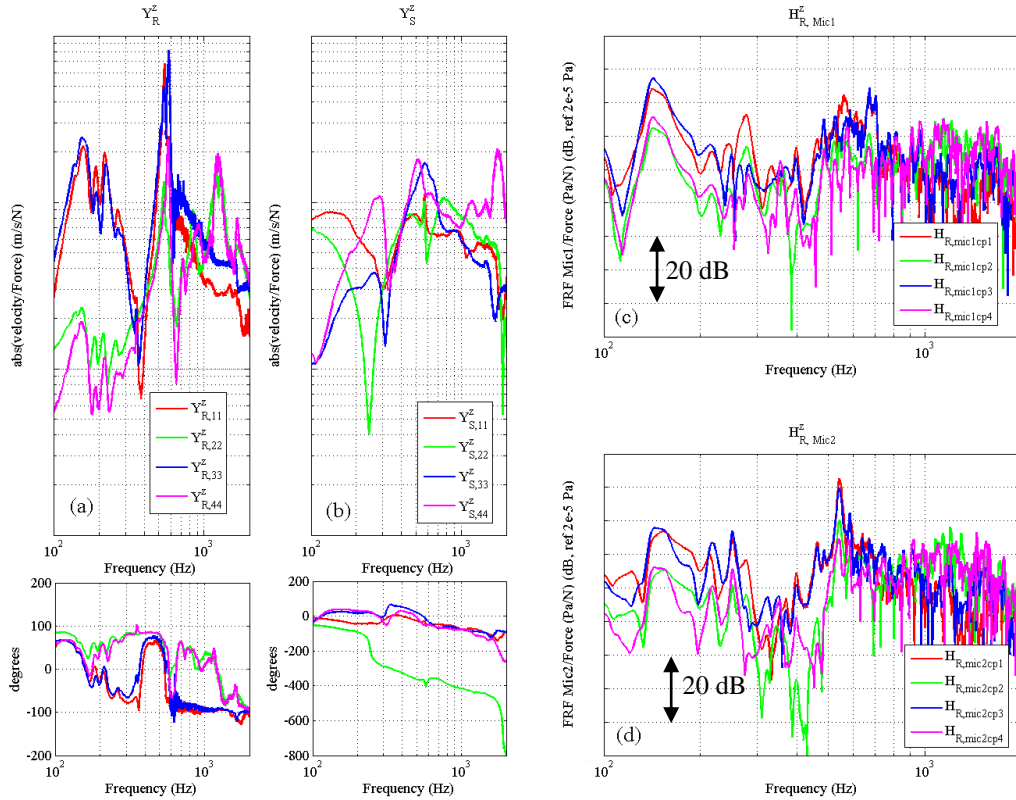


Fig. 3 – (a) Receiver structure Point mobility (z component), (b) Source point mobility (z component), (c) Vibroacoustic transfer function at Microphone 1, (d) Vibroacoustic transfer function at Microphone 2.

Vibroacoustic transfer function

For each impact applied to the receiver structure during the characterization of \mathbf{Y}_R , the transfer function \mathbf{H}_R between the microphones and the force applied by the impact hammer was recorded. \mathbf{H}_R , of dimension $[12 \times 1]$ in the proposed configuration, will be used to predict the SBN according to Eq. (7). Figure 3(c) and 3(d) show, respectively, the vibroacoustic transfer function recorded at microphones 1 and 2 when an impact force is applied at connection points along the z direction. The behavior recorded at both microphones is similar. For frequencies up to 800 Hz, the mechanical energy applied at points CP1 and CP3 is more easily transferred to acoustical energy in the cavity compared to points CP2 and CP4. Above this frequency, all connection points contribute similarly.

3.3 Source characterization

Free velocity

The free velocity at the four connection points is measured when the source is “freely” suspended (see Fig. 2(c)). A tri-axial accelerometer was placed on each connection point in order to record the acceleration along x , y and z simultaneously. The three components of the free velocity measured at each connection points are shown in Figure 4. Two main peaks can be observed at 120 Hz and 155 Hz and can be observed in the three directions. The x -contribution at 120Hz is however largely inferior to the y - and z - contributions. Above 500 Hz, the z -contribution slightly dominates at all connection points.

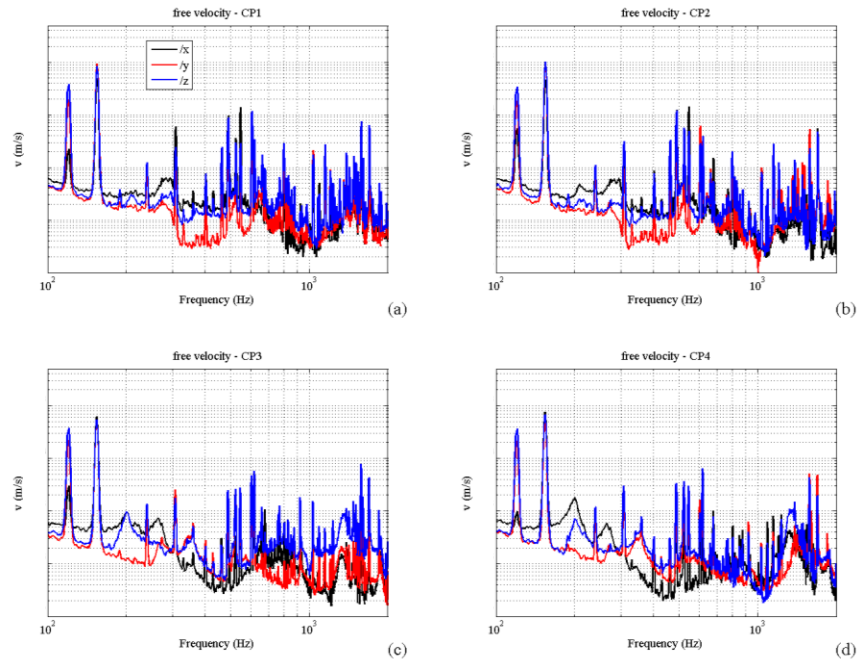


Fig. 4 – (a) x , y , and z components of the connection points Free velocity measured when the source is suspended; (a) CP1, (b) CP2, (c) CP3, (d) CP4.

Blocked force

As mentioned previously, no rigid structure was available during the measurement campaign and thus the blocked force could not be measured using the direct method. It is estimated in this work from the source free velocity and source mobility matrix according to Eq. (2). Figure 5 presents the operational force of the hard-mounted source derived from Eq. (5) and the blocked force derived from Eq. (2). The free velocity is thus involved in both calculations. For frequencies above 300 Hz, the operational force and the blocked force are very similar. Below 300 Hz, the operational force is inferior to the blocked force and more particularly for connection points CP3 and CP4. According to Eq. (6), the difference observed between F_R and F_B can be attributed to the relative difference between Y_R and Y_S : F_R is inferior to F_B at a given contact point when the structure mobility dominates over source mobility (i.e., $Y_S / (Y_S + Y_R) < 1$).

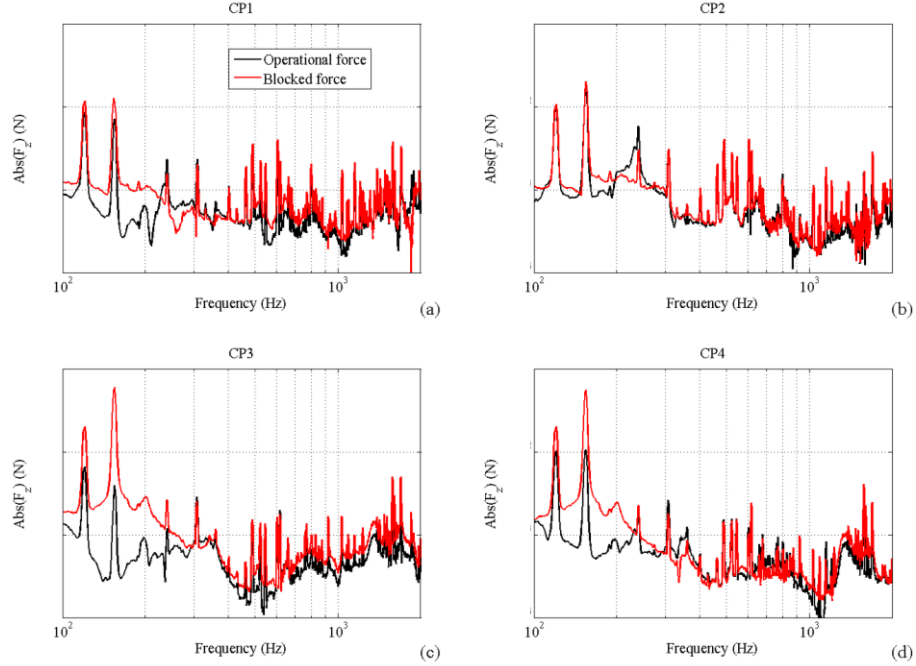


Fig. 5 – z component of the blocked force and operational force estimated at the connection points; (a) CP1, (b) CP2, (c) CP3, (d) CP4.

3.4 SBN generated in the cavity

The SBN in the cavity is now computed from Eqs. (5), (7) and (8). The calculation is carried out while accounting for the contribution of all components (x , y and z) and by the contribution of each component separately. As mentioned previously, the coupling between components is neglected (see zeros in the matrix of Eq. (1)). Furthermore, the impact of moments and angular displacements are also neglected.

The results of the hard-mounted source configuration are presented in Figure 6. SBN predictions are compared with measurements obtained from Eq. (9) (see grey line). The upper figure present the results in the whole frequency range of interest. Figures at the bottom shows zoom in specific frequency range where SBN peaks having significant amplitude can be observed. The focus will be on these peaks with an emphasis on the first two peaks at 120 Hz and 155 Hz, since they carry most the vibratory energy. It is shown that the main peak at 155 Hz is correctly predicted when the three translational degrees of freedom are accounted for (see red curve): the predicted amplitude is only 2 dB below the measured one. This difference is acceptable considering the multiple assumptions made along this work. If only the z - or the y -components are taken into account (see blue and green curves respectively), the estimated peak amplitude is found 5 dB lower than the measured one. Finally, this peak is highly underestimated if only the x -component is taken into account (the maximum of the peak is 14 dB lower in amplitude). It can be concluded that, in this configuration, both the y - and z - components have to be accounted for. In the rest of the frequency range (see zooms 2 and 3 in Figure 6), it is shown that the peak amplitude is slightly underestimated (≈ 5 dB) even if all components are taken into account. This can be attributed to (1) the neglected rotational degrees of freedom and (2) the neglected transfer mobilities between components (x , y and z). Furthermore, it appears that the normal translational degrees of freedom (along z) mainly contributes to SBN from mid to high

frequencies since the SBN predicted by the component only is almost superimposed with the one computed with the three components.

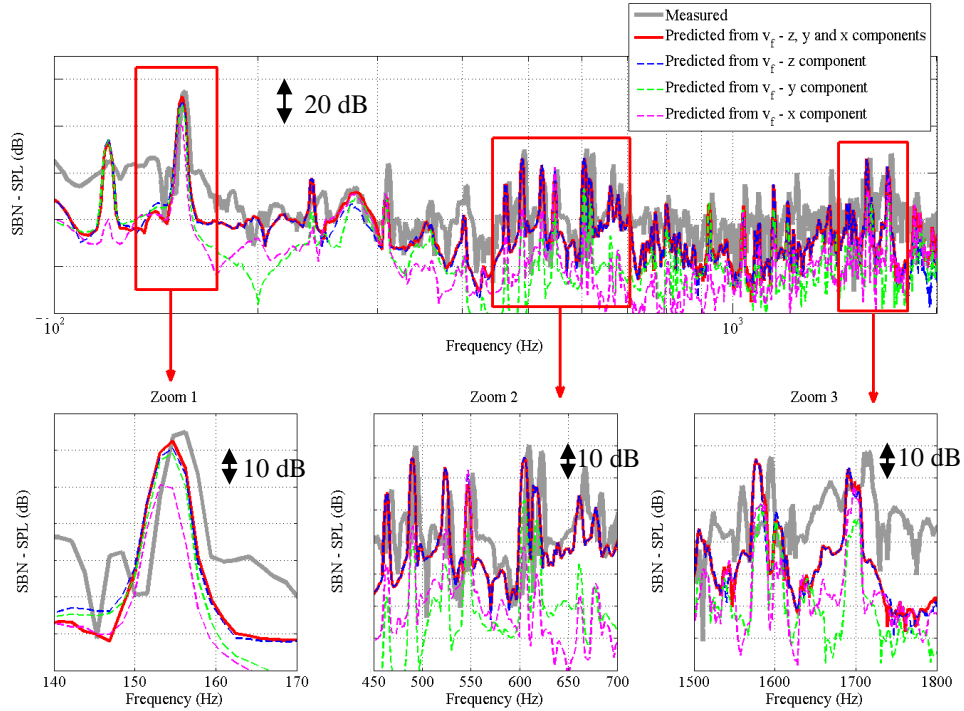


Fig. 6 – Structure-borne noise at microphone 1; case of the hard-mounted source.

Figure 6 also shows that the peak predicted at 120 Hz (due to the important free velocity measured at all connection points at this frequency, see Fig. 4) barely appears in the SBN measurement and that the measured SBN_m is significantly higher than SBN_T for $f < 200$ Hz (except at the 120 Hz and 155 Hz peaks). These discrepancies in the predictions could be attributed to the fact that the vibratory behavior of the coupled system cannot be predicted as accurately as expected from the vibratory behaviors of the uncoupled sub-structures. Considering such light receiver structure (sharing similar mobilities with the selected source), the coupled modes of the assembly can be significantly different from the modes of the independent sub-structures. In this case, a characterization of the operational force from the coupled structure could be more appropriate⁹.

4 CONCLUSIONS

The objective of this paper was to investigate the potential of a well-known SBN characterization method for light structures as encountered in aircrafts and coupled to realistic aircraft equipment. The method applied in this work is based on the characterization of source and receiver properties measured independently. All aforementioned properties are then combined using straightforward analytical expressions and coupled to vibroacoustic transfer functions in order to assess the SBN in a given acoustic domain. Only the translational degrees of freedom are accounted for in order to propose a simple and practical method. The structure-borne method is tested from a small scale laboratory setup comprising of an avionic fan mounted onto an aluminum structure which is then coupled with a small reverberant chamber. The fan produces two main tonal forces at 120 Hz and 155 Hz and generates a high SBN in the cavity

mainly at 155 Hz. The structure-borne method allows to correctly predicting the SBN peak at 155 Hz provided that at least the two force components in the plane orthogonal to the rotating shaft (y and z in this work) are accounted for. The amplitude of the peaks of the harmonics at higher frequencies is also correctly predicted. However, large discrepancies can be observed for frequencies below 140 Hz. These discrepancies could be attributed (1) to the strong modification of the vibratory behavior when the sub-structures are coupled (independent sub-structure characterization cannot be suitable in this frequency range) and/or (2) to the accuracy of the mobility measurements of the suspended source. This low frequency issue and the effect of soft mounts are perspectives of the current work.

5 REFERENCES

1. M. Lievens, "Structure-borne sound sources in buildings", PhD thesis, Aachen University (2013).
2. S. Helderweirt, H. V. der Auweraer, and P. Mas. "Application of accelerometer-based rotational degree of freedom measurements for engine subframe modelling", IMAC XIX - 19th International Modal Analysis Conference, (2001).
3. H.Y.K. Lai, "Integrated reception-plate inverse-force test method for commercial airplane equipment structure-borne noise specification and qualification", proceedings of Internoise, New York, (2012).
4. L. Cremer, M. Heckl and B.A.T. Petersson, *Structure-Borne Sound: Structural Vibrations and Sound Radiation at Audio Frequencies*, 3rd edition, Springer Berlin Heidelberg New York; Chap. 5.8.5 "Vibration transmission from Machinery", pp. 326-340, (2005)
5. F. Fahy and J. Walker, *Advanced applications in acoustics, noise and vibration*, Spon Press, London and New York (2004); Chap. 9, written by P. Gardiono and M.J. Brennan, "Mobility and impedance methods in structural dynamics, pp.406-410, (2004)
6. International Standards Organisation ISO 7626-5, Vibration and shock - Experimental determination of mechanical mobility - Part 5: Measurements using impact excitation with an exciter which is not attached to the structure, (1994).
7. International Standards Organisation ISO 7626-2, Vibration and shock - Experimental determination of mechanical mobility - Part 2: Measurements using single-point translation excitation with an attached vibration exciter, (1990).
8. International Standards Organisation ISO 9611, Acoustics characterisation of sources of structure-borne sound with respect to sound radiation from connected structures - measurement of velocity at the contact points of machinery when resiliently mounted, (1996).
9. A.T. Moorhouse, A.S. Elliott and T.A. Evans, "In situ measurement of the blocked force of structure-borne sound sources", *Journal of Sound and Vibration* 325, pp. 679-685, (2009).